Jurnal Sains Nuklear Malaysia, 2017, 29(2): 1 – 9
ISSN: 2232-0946

NUMERICAL EXPERIMENTS TO STUDY THE VARIATION OF PRESSURE ON INDIA BHABHA ATOMIC RESEARCH CENTRE PLASMA FOCUS

Arwinder Singh[1], Saw Sor Heoh[2,3] and Lee Sing[1,2,3,4]

[1]INTI International University, 71800 Nilai, Negeri Sembilan, Malaysia
[2]Nilai University, 71800 Nilai, Negeri Sembilan, Malaysia
[3]Institute for Plasma Focus Studies, Australia
[4]University of Malaya, Kuala Lumpur, Malaysia
Correspondence author: arwinders.jigiris@newinti.edu.my

ABSTRACT

In this paper a study on the relationship between axial speed v_a, *radial shock speed* v_s, *piston speed* v_p *and pinch temperature with the variation of pressure* P_0 *was carried out. The Lee's 5 phase model code was used in this study by configuring the India Bhabha Atomic Research Center (BARC) plasma focus machine to operate in the pressure* (P_0) *range from 1 Torr to 14 Torr. The relationships between these parameters were obtained as follows:*

$$v_a \approx 9P_0^{-0.37}, v_s \approx 45P_0^{-0.48}, v_p \approx 30P_0^{-0.47} \text{ and } T_{pinch\ (max)} \approx 11P_0^{-1}$$

Keywords: Axial velocity, dense plasma focus, neutron yield, numerical experiment, Lee model code, radial trajectories

INTRODUCTION

The dense plasma focus machine produces by means of electromagnetic acceleration and compression (during pinching) short live plasma that can be used to study nuclear fusion in plasmas. To understand the performance of a plasma focus machine, the current trace (Lee and Saw, 2010a), should be analysed because it contains information on the dynamic, electrodynamic, thermodynamic and radiation processes that occur in the various phases of the plasma focus (Lee, 1984; Lee, 1985; Lee and Saw, 2010b). One of the most important procedures therefore is to connect the numerical experiment (Lee, 2014) to the reality of the actual machine by fitting the computed current trace to a measured current trace (Lee, 2009; Lee et al., 2009; Lee and Saw, 2008; Lee and Saw, 2010a; Lee and Saw, 2012; Saw and Lee, 2010; Saw and Lee, 2011). This methodology is employed in this paper to obtain the relationship between the axial speed, radial shock speed, piston speed and pinch temperature with the variation of pressure working in deuterium gas for the BARC plasma focus machine. The computed and measured neutron yield for this machine is also compared and discussed.

PROCEDURE FOR NUMERICAL EXPERIMENT

The machine parameters of the 11.5 kJ India Bhabha Atomic Research Center (BARC) plasma focus machine is as follows (Niranjan, 2015). The BARC plasma focus machine is a conventional Mather (Marshal, 1960) type squirrel cage geometry machine. The electrode structure of this machine consists of a stainless steel anode tube 77 mm long, 60 mm in diameter while the outer cathode consists of twelve, 12 mm diameter rods uniformly spaced coaxially at a diameter of 122 mm. The anode and cathode are made of stainless steel (SS304 material) which is separated by

insulator made of quartz having a thickness of 2 mm. A triggered spark gap switch is connected to a capacitor bank consisting of four capacitors (10 µF each capacity) connected in parallel to a common collector plate. This 40 µF capacitor was charged to 24 kV and operated in deuterium. An average of 10 shots at different pressure was taken and the amount of neutron yield produce was measured using a silver activation detector counts.

The measured data of current trace and neutron yield of the BARC PF was kindly provided by Rout (2013). We then used the Lee's 5 phase model code (Lee, 2017; Lee et al., 1998; Lee et al., 2014) (version: RADPF5.15) to configure the BARC plasma focus machine to fit a current trace obtained at 3 Torr by entering the machine, operation and fitting parameters as shown in Table 1.

Table 1: Machine, operation and fitting parameters for the BARC plasma focus machine used for this numerical experiment

Capacitance C_0 (µF)	40
Static inductance L_0 (nH)	77
Circuit resistance r_0 (mΩ)	4
Cathode radius 'b' (cm)	6.1
Anode radius 'a'(cm)	3
Anode length 'z_0'(cm)	7.7
Charging voltage V_0 (kV)	24
Fill gas pressure P_0 (Torr)	3
Fill gas (molecular weight)	4
Fill gas (atomic number)	1
Fill gas (molecule (2))	2
Axial phase mass factor, f_m	0.22
Axial phase current factor, f_c	0.7
Radial phase mass factor, f_{mr}	0.22
Radial phase current factor, f_{cr}	0.72

RESULTS

The computed and measured current traces in Figure 1 show a good fit. The peak current computed is 446 kA and exhibits a radial phase start time of 2.113 µs for pinch duration of 0.246 µs with a neutron yield of 1.04×10^9 n. The computed values of the maximum pinch temperature, axial and radial speed as well as the neutron yield at 24 kV, 3 Torr deuterium gas are presented in Table 2.

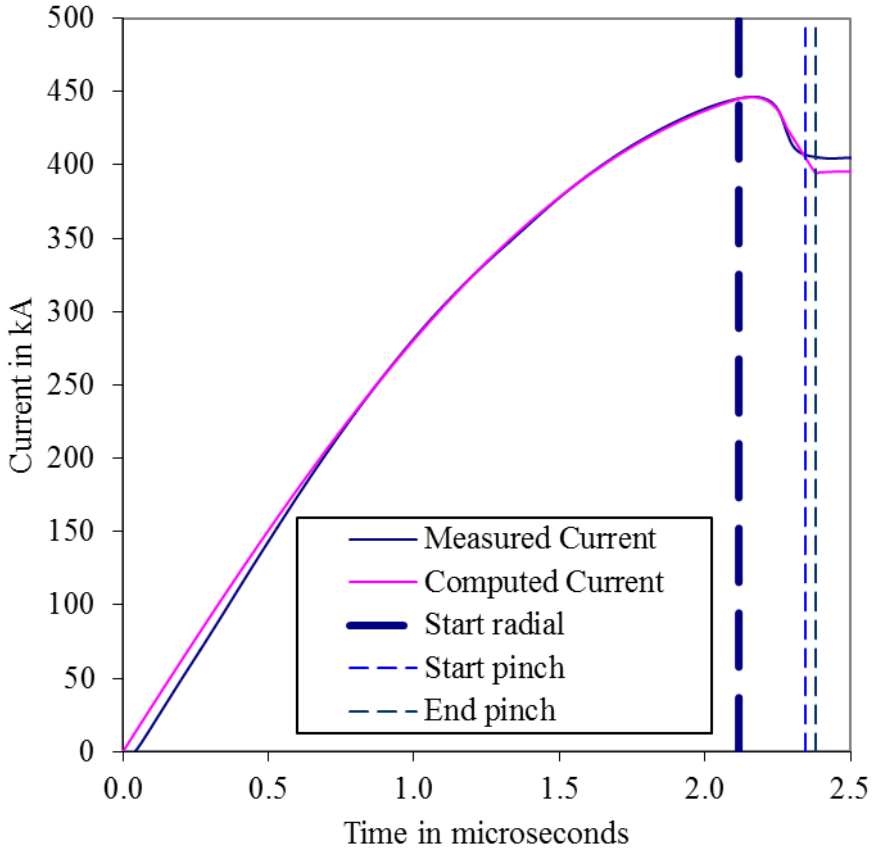

Figure 1: The measured current trace obtained from the current derivative of the BARC plasma focus machine at 24 kV, 3 Torr deuterium gas compared with computed current trace obtain using the Lee's 5 phase model code

Table 2: Information obtained from Lee's 5 phase model code configured for the BARC plasma focus machine at 24 kV, 3 Torr deuterium gas

Pinch maximum temperature (10^6 K)	3.75
Peak axial speed (cm/μs)	6.3
Peak radial shock speed (cm/μs)	27.2
Peak radial piston speed (cm/μs)	18.5
Neutron yield (10^9 n)	1.04

Using the machine operation and the fitted model parameters as shown in Table 1, the BARC plasma focus machine is now configured at 24 kV, deuterium for pressure ranging from 1 Torr to 14 Torr to study the effect of the variation of pressure on maximum pinch temperature as well as the axial, radial and piston speeds. From the computed output we plotted Figures 2 − 5.

When computed axial speed (v_a) was plotted in log scale against the variation in pressure P_0 as shown in Figure 2, we obtained the formula $v_a = 9.304P_0^{-0.369}$ where the axial speed is in cm/μs while the pressure is in Torr. This can be approximated as $v_a \approx 9P_0^{-0.37}$.

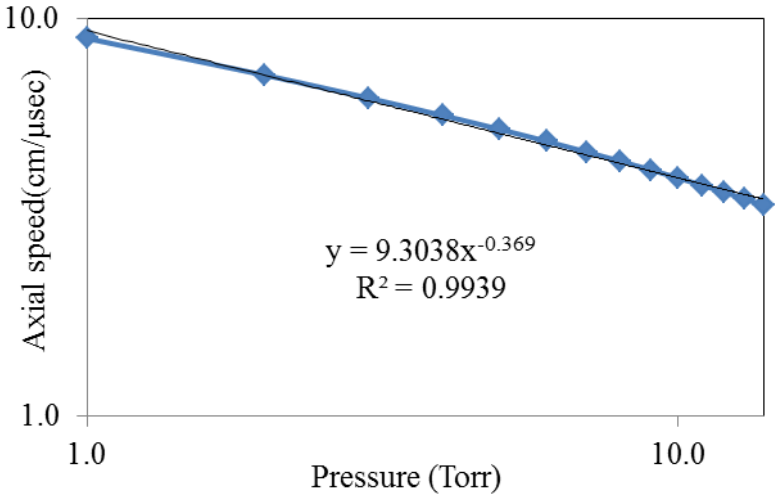

Figure 2: The variation of computed axial speed with respect to pressure operating at 24 kV in deuterium for the BARC plasma focus machine

The computed axial phase of the Lee code uses an electromagnetic snowplow mechanism to compute the axial speed. Such a mechanism invariably produces an axial speed which is proportional to $(I/a)/P_0^{0.5}$; this quantity being known as S, the speed factor (Lee and Serban, 1996). From this dependence it would seem at first sight that operating at the same voltage with the same anode radius one would expect that the axial speed being proportional to speed factor S should be proportional to pressure (the density ρ_0 being proportional to P_0). However the circuit equation is coupled to the current sheath motion through what is essentially the motor back electromotive force EMF effect. This back EMF effect requires that the faster the current sheath moves, the greater the back EMF which reduces the magnitude of the current. Thus as operational pressure is increased the circuit current increases due to slower current sheath speed. This provides a small compensation to the drop in speed due to the greater mass loading. This explains why the dependence of v_a with P_0 is not to the power of -0.5, but rather to a lesser power of -0.37.

When computed radial inward shock speed (v_s) and radial piston speed (v_p) were individually plotted in log scale against P_0 as shown in Figures 3 and 4, respectively, we obtained the formula $v_s = 44.542P_0^{-0.481}$ and $v_p = 30.035P_0^{-0.468}$ respectively where the radial inward shock speed v_s and radial piston speed v_p are in cm/µs while the pressure P_0 is in Torr. This can be approximated as $v_s \approx 45P_0^{-0.48}$ and $v_p \approx 30P_0^{-0.47}$. The radial phase of the code uses an electromagnetic slug model mechanism to compute the radial speed (Lee, 2014). The speed of the radial inward shock speed is determined by the magnetic pressure whereas the speed of the piston is determined by the first law of thermodynamics applied to the effective increase in volume between the shock front and the current sheet which is created by the incremental motion of the shock front.

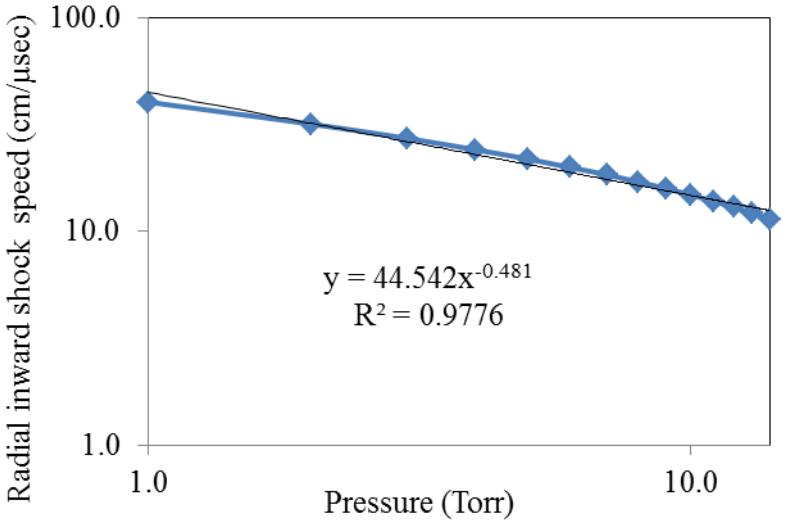

Figure 3: The variation of computed radial inward shock speed with respect to pressure operating at 24 kV in deuterium for the BARC plasma focus machine

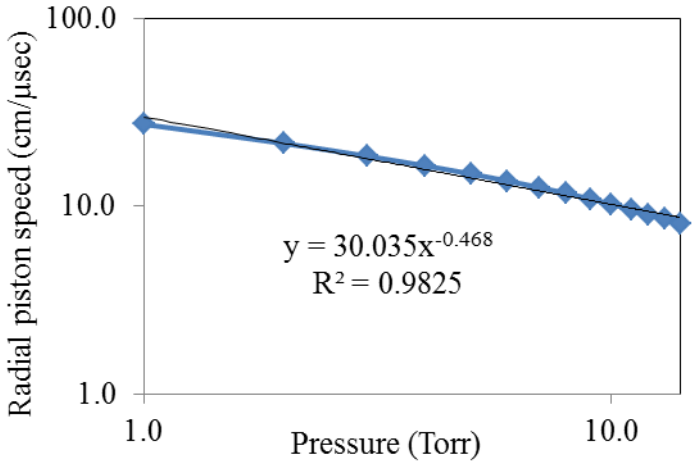

Figure 4: The variation of computed magnetic piston speed with respect to pressure operating at 24 kV in deuterium for the BARC plasma focus machine

When the computed maximum pinch temperature ($T_{pinch\ (max)}$) was plotted in log scale against the variation in pressure P_0 as shown in Figure 5, we obtained the formula $T_{pinch\ (max)}=10.635\,P_0^{-1.021}$ where the pinch temperature is in 10^6 K (10^6 Kelvin) and the pressure P_0 is in Torr. This can be approximated as $T_{pinch(max)} \approx 11P_0^{-1}$. The detail explanation for this graph will be discussed in the next paragraph.

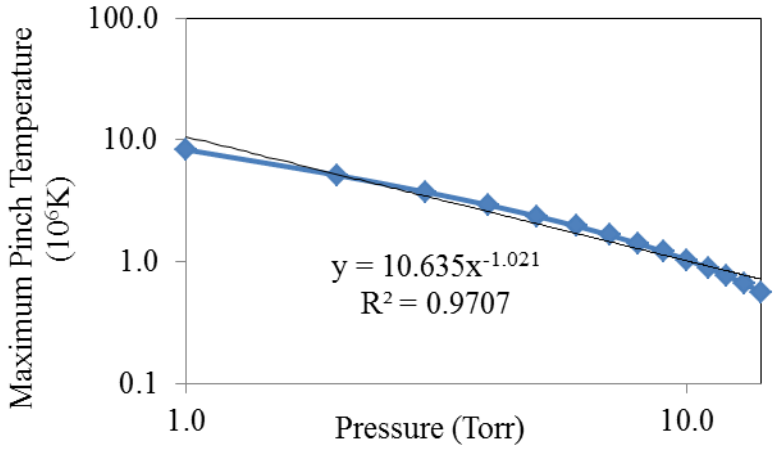

Figure 5: The variation of maximum pinch temperature with respect to pressure operating at 24 kV in deuterium for the BARC plasma focus machine

DISCUSSION

Using the information obtained from the above Figures 2 − 5, it can be noted that as the pressure P_0 increases the axial speed v_a decreases. Similarly the radial shock speed v_s and the radial magnetic piston speed v_p also decreases. The decrease in the radial shock speed v_s causes a decrease in the temperature of the inward radial shock (the temperature depends on the shock speed to power of 2). This sets the stage for a decreased pinch temperature as pressure P_0 increases. As these two radial speed decreases, the time required for the radial reflected shock increases and also the pinch duration increases.

From Figure 2, we note that at around 6 Torr (at an axial speed around 5 cm/μs) there seems to be a gradual transition to a faster drop in speed than at lower pressures as can be observed by the closeness of these data points. The cause of this deviation is clear when we note that in the range up to 6 Torr, the end of the axial phase occurs at a time of 0.4 μs on either side of the peak current which occurs at 2.3 μs. Thus the axial phase ends with the drive current near the peak value of 450 kA. At 6 Torr and higher pressures, the end of the axial phase occurs progressively further and further from the peak current, thus the drive current is reduced to lower values, around 300 kA for the 6 Torr case. This reduction in drive current (due to shifting the end point of the radial phase further and further away from time of peak current) accentuates the decrease in end axial speed, causing the deviation from the straight line in the log-log curve.

The radial shock speed is related to the axial speed by a predominantly geometrical factor which is about 2 for this plasma focus. Thus the same transition (to faster drop with P) is seen also in the behavior of the radial shock speed in Figure 3. The radial piston speed is related to the radial shock speed and a similar transition is seen in Figure 5 for the radial piston speed behaviour. The temperature (with a squared dependence on the radial shock speed) likewise shows the same, albeit accentuated, transition starting around 6 Torr.

When the measured and computed neutron yield versus variation in pressure P_0 was plotted as shown in Figure 6, the maximum computed neutron yield of 1.63×10^9 n occurred when the pressure was 7 Torr as compared to the maximum experimental yield of $(1.28 \pm 0.3) \times 10^9$ n that occurs at 3 Torr. From Figure 6, it can be seen that the experimental and computed result are peak values are

reasonably close (factor of 1.2 for the point showing the biggest difference) even though the experimental values are at lower pressure as compared to the computed values. This difference between the measured optimum pressure and the computed optimum pressure is noted in several previous comparisons (Lee et al., 2009). One possible cause of the discrepancy is the use of fixed model parameters (based on the fitted model parameters at one pressure, in this series at 3 Torr) in the computation over the range of pressures. The model parameters particularly the mass factors dictated by the mass actually swept-up by the magnetic piston (Chow et al., 1972; Tou et al., 1989) may likely vary significantly with the pressure. A better comparison would be to fit a current trace at each pressure to obtain the model parameters to be used in the code at each pressure. However this is usually not possible as in this case since only a representative measured current trace is available, in this case for the shot at 3 Torr.

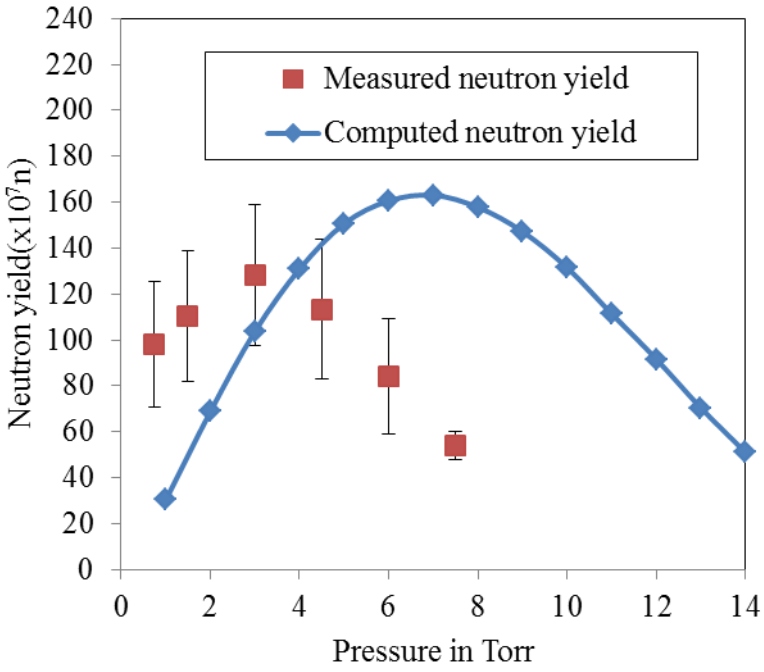

Figure 6: The variation of computed and experimental neutron yield with respect to pressure operating at 24 kV in deuterium for the BARC plasma focus machine

CONCLUSIONS

From these numerical experiments, we can conclude that for the BARC plasma focus machine, the variation of operational pressure P_0 with axial speed v_a, radial shock speed v_s, piston speed v_p and pinch temperature has the relationship as shown below.

$$v_a \approx 9P_0^{-0.37}$$

$$v_s \approx 45P_0^{-0.48}$$

$$v_p \approx 30P_0^{-0.47}$$

and $$T_{pinch\ (max)} \approx 11P_0^{-1}$$

The result of the computed neutron yield also agrees reasonably well with the experimental yield (Rout, 2013) which gives us the confidence that not only the Lee 5-phase model code computes the optimum neutron yields but also the dynamic behavior of the plasma pinch in respect to the variation in pressure.

REFERENCES

Chow, S.P., Lee, S. and Tan, B.C. (1972). Current sheath studies in a co-axial plasma focus gun, *J. Plasma Phys.* 8: 21-31.

Lee, S. (1984). Radiation in plasma. In: Namara, B. (Ed.), *World Scientific, Singapore*, Vol II, pp. 978.

Lee, S. (2014). Plasma focus Radiative Model-Review of the Lee Model code, *J. Fusion Energy* 33: 319-335.

Lee, S. (2017). Radiative dense plasma focus computation package: RADPF, 2017. http://www.plasmafocus.net

Lee, S. and Saw, S.H. (2008). Neutron scaling laws from numerical experiments, *J. Fusion Energy* 27(4): 292-295.

Lee, S. and Saw, S.H. (2010a). The plasma focus-scaling properties to scaling laws, *Joint ICTP-IAEA Workshop on Dense Magnetized Plasma and Plasma Diagnostics*, 15 - 26 November 2010.

Lee, S. and Saw, S.H. (2010b). Numerical experiments providing new insights into plasma focus fusion devices, *Energies* 3(4): 711-737.

Lee, S. and Saw, S.H. (2012). The plasma focus-trending into the future, *Int. J. Energy. Res.* 36(15): 1366-1374.

Lee, S. and Serban, A. (1996). Dimensions and lifetime of the plasma focus pinch, *IEEE Transactions on Plasma Science* 23(3): 1101-1105.

Lee, S., Saw, S.H., Hegazy, H., Jalil Ali, Damideh, V., Fatis, N., Kariri, H., Khubrani, A. and Mahasi, A. (2014). Some generalised characteristics of the electro dynamics of the plasma focus in its axial phase-illustrated by an application to independently determine the drive current fraction and the mass swept-up fraction, *J. Fusion Energy* Published online 5 Jan 2014.

Lee, S., Saw, S.H., Soto, L., Springham, S.V. and Moo, S.P. (2009). Numerical experiments on plasma focus neutron yield versus pressure compared with laboratory experiments, *Plasma Phys. Control. Fusion* 51: 075006-0750011.

Lee, S., Tou, T.Y., Moo, S.P., Eissa, M.A., Gholap, A.V., Kwek, K.H., Mulyodrono, S., Smith, A.J., Suryadi, Usada, W. and Zakaullah, M. (1998). A simple facility for the teaching of plasma dynamics and plasma nuclear fusion, *Am. J. Phys.* 56(1): 62-68.

Lee. S. (1985). Laser and plasma technology. In: Lee, S., Tan, B.C., Wong, C.S. and Chew, A.C. (Eds.), *World Scientific, Singapore*, pp. 37, 64 and 387.

Lee. S. (2009). Neutron yield saturation in plasma-focus: A fundamental cause, *Appl. Phys. Lett.* 95 (15): 151503-151533.

Marshall, J. (1960). Performance of a hydromagnetic plasma gun, *Phys. Fluids.* 3(1): 134-135.
Niranjan, R., Rout, R.K., Srivastava, R., Chakravarthy, Y., Mishra, P., Kaushik, T.C. and Gupta, S.C. (2015). Surface modifications of fusion reactor relevant materials on exposure to fusion grade plasma in plasma focus device, *Appl. Surface Sci*. 355: 989-998.

Rout, R.K. (2013). Private communication, India Bhabha Atomic Research Center, 18 December 2013.

Saw, S.H. and Lee, S. (2010). Scaling laws for plasma focus machines from numerical experiments, *Energy and Power Engineering*, pp. 65-72.

Saw, S.H. and Lee, S. (2011). Scaling the plasma focus for fusion energy considerations, *Int. J. Energy Res.* 35: 81-88.

Tou, T.Y., Lee, S. and Kwek, K.H. (1989). Nonperturbing plasma-focus measurements in the run-down phase, *IEEE Trans. Plasma Sci*. 17(2): 311-315.